ACS MATERIALS LETTERS

Cite This: ACS Materials Lett. 2020, 2, 71−75

www.acsmaterialslett.org

LETTER

Crystal Synthesis and Frustrated Magnetism in Triangular Lattice Cs*RE*Se$_2$ (*RE* = La−Lu): Quantum Spin Liquid Candidates CsCeSe$_2$ and CsYbSe$_2$

Jie Xing,*[,∇,†] Liurukara D. Sanjeewa,[∇,†] Jungsoo Kim,[‡] G. R. Stewart,[‡] Mao-Hua Du,[†] Fernando A. Reboredo,[†] Radu Custelcean,[§] and Athena S. Sefat*[,†]

[†]Materials Science and Technology Division, Oak Ridge National Laboratory, Oak Ridge, Tennessee 37831, United States

[‡]Department of Physics, University of Florida, Gainesville, Florida 32611, United States

[§]Chemical Sciences Division, Oak Ridge National Laboratory, Oak Ridge, Tennessee 37831, United States

Supporting Information

ABSTRACT: **A triangular lattice selenide series of rare earths (*RE*), Cs*RE*Se$_2$, were synthesized as large single crystals, using a flux growth method. This series stabilized in either trigonal (*R*3*m*) or hexagonal (*P*6$_3$/*mmc*) crystal systems. Physical properties of Cs*RE*Se$_2$ were explored by magnetic susceptibility and heat capacity measurements down to 0.4 K. Antiferromagnetic interaction was observed in all magnetic compounds, while no long-range magnetic order was found, indicating the frustrated magnetism. CsDySe$_2$ presents spin freezing at 0.7 K, revealing a spin-glass state. CsCeSe$_2$ and CsYbSe$_2$ present broad peaks at 0.7 and 1.5 K, respectively, in the magnetization, suggesting the short-range interactions between magnetic *RE* ions. The lack of signature for long-range magnetic order and spin freezing down to 0.4 K in these compounds (*RE* = Ce, Yb) implies their candidacy for a quantum spin liquid state.**

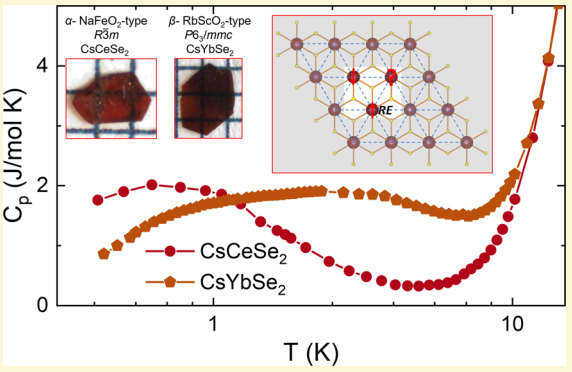

The topic of quantum spin liquid (QSL) has been attracting a great amount of interest, because of its potential application for future quantum communication and computation.[1−4] The highly entangled spins in QSL remain dynamic, even at zero temperature, without breaking any symmetry. The frustrated magnetic materials with degenerate ground states are excellent candidates for QSL. To date, some organic and inorganic transition-metal-containing triangular magnetic lattices such as κ-(BEDT-TTF)$_2$Cu$_2$(CN)$_3$, EtMe$_3$Sb[Pd(dmit)$_2$]$_2$, Ba$_3$CoSb$_2$O$_9$, Ba$_8$CoNb$_6$O$_{24}$, and NaTiO$_2$ are proposed to have interesting magnetic ground states, revealed by theoretical calculations and experimental results.[5−13] At the same time, frustrated magnetic lattices with rare-earth (*RE*) ions have been attractive, because of the large spin-orbital coupling and anisotropic magnetic interaction.[14] Moreover, triangular magnetic lattices with *RE* ions exhibit diverse magnetic ground states.[15,16] For example, *RE* ions with an odd number of 4*f* electrons (i.e., Kramer ions) could be treated as having an effective spin J_{eff} = 1/2. One of the famous materials is YbMgGaO$_4$ in which Yb^{3+} ions form a triangular magnetic lattice, and it was proposed, by experiments and theory, as a QSL candidate.[17−21]

Recently, a large class of compounds with the formula of *ARE*Q$_2$ (where A = Na, K, Rb and Cs, and Q = O, S, Se, and Te) has been proposed as QSL candidates.[22−26] Because of the different sizes of A-site cations, *RE* ions, and *Q*, *ARE*Q$_2$ (112) is a special class of compound that has a tendency to crystallize in different crystal space groups: LiLaO$_2$ in *P*2$_1$/*c*, LiEuO$_2$ in *Pbm*, LiYbO$_2$ in *I*4$_1$/*amd*, NaTbO$_2$ in *C*2/*c*, NaYbO$_2$ in *R*3̄*m*, CsNdO$_2$ in *P*6$_3$/*mmc*, and NaLaS$_2$ in *Fm*3̄*m*.[27−36] Among these 112-class compounds, high symmetry structures maintain perfect *RE* triangular lattices that are separated by the A-site cations. These compounds crystallize without any disorder formation, unlike the mixed occupation of Mg and Ga atoms in YbMgGaO$_4$, which may facilitate a disordered state similar to a spin liquid state.[37−39] Dzyaloshinskii−Moriya interaction is

Received: November 6, 2019
Accepted: November 26, 2019
Published: November 26, 2019

DOI: 10.1021/acsmaterialslett.9b00464
ACS Materials Lett. 2020, 2, 71−75

prohibited due to the magnetic *RE* ions occupying the high-symmetry sites in these compounds, similar to QSL candidate $YbMgGaO_4$.[18,40−42] Hence, 112-type compounds with triangular layers are an open ground to investigate novel frustrated magnetism.

However, among this 112 class of compounds, several important challenges remain, including limited known compounds and difficulty of growing large single crystals for finding anisotropic magnetic properties. These can be well-exemplified by the Cs*RE*Se_2 family. So far, only the structure of $CsYbSe_2$ was reported, which was synthesized via complex multiple steps.[43] In this work, we employed a new and simple flux method to grow large single crystals of 112-class compounds, enabling anisotropic physical property measurements and inelastic neutron scattering experiments. In addition, for the first time, we confirmed that new compounds in this Cs*RE*Se_2 series crystallize in either trigonal or hexagonal crystal systems, depending upon the size of the RE^{3+} ion.

The Cs*RE*Se_2 compounds were synthesized via an easy two-step method: first, the powder form of the target phase is synthesized using the stoichiometric amounts of the elements as starting materials; second, this precursor was mixed with the CsCl salt flux to obtain single crystals. More details of the synthesis procedure are given in the Supporting Information (SI). For the first time, we report that large high-quality single crystals of Cs*RE*-based 112-class compounds can be synthesized using this technique, as shown in Figure 1. In addition, we report the single-crystal structure characterization (details are given in the SI) and anisotropic magnetic properties of the Cs*RE*Se_2 series (*RE* = La−Lu).

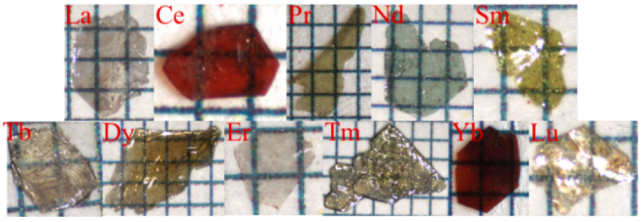

Figure 1. Single crystals of Cs*RE*Se_2 grown using a salt flux. The grid is in 1 mm scale; the *c*-axis is projecting out of the page.

We find that the Cs*RE*Se_2 series adopts two crystal systems: trigonal $R\bar{3}m$ types (α-$NaFeO_2$) and hexagonal $P6_3/mmc$ types (β-$RbScO_2$). Cs*RE*Se_2 with larger RE^{3+} ionic radii (La, Ce, Pr, Nd, and Sm) are iso-structural and possess α-$NaFeO_2$ structure type, while Cs*RE*Se_2 with smaller RE^{3+} ionic radii (*RE* = Tb, Dy, Er, Tm, Yb, and Lu) form hexagonal β-$RbScO_2$ structure type. A comparison of these two structure types is presented in Figure 2. In both structures, each of the Cs, *RE*, and Se atoms has a special position. In the α-$NaFeO_2$ structure type, Cs (Wyckoff 3*b*) and *RE* (3*a*) sites have $\bar{3}m$ symmetry, while Se (6*c*) has 3*m* site symmetry. In comparison, in the β-$RbScO_2$ structure type, Cs (2*c*) and *RE* (2*b*) sites are in $\bar{6}m2$ and $\bar{3}m$ special positions, respectively, while Se (4*f*) is in the 3*m* position. This obvious structural change among this Cs*RE*Se_2 family is likely due to the slight deviation of the RE^{3+} ionic radii, which is supported by DFT calculation (see the SI). Visually, the α-$NaFeO_2$ and β-$RbScO_2$ structure types exhibit different packing along the *c*-axis, as shown in Figure 2; herein, the atomic arrangement of one-unit cell of each of $CsLaSe_2$ and $CsTbSe_2$ is used to compare these differences. In $CsLaSe_2$, three layers of La−Se−La are packed along the *c*-axis, while

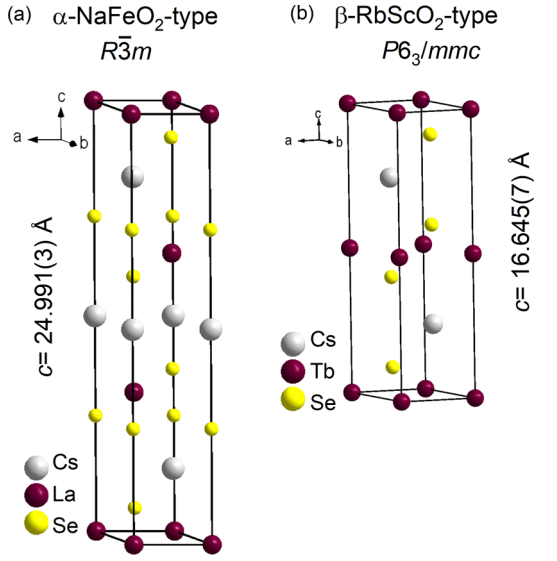

Figure 2. (a) Structure showing packing of Cs, La, and Se atoms in $CsLaSe_2$ structure that crystallizes in the α-$NaFeO_2$-type. (b) Packing of Cs, Tb, and Se atoms in $CsTbSe_2$ structure that crystallizes in the β-$RbScO_2$ type.

only two layers of Tb−Se−Tb are packed in $CsTbSe_2$. In both cases, each *RE*Se_6 octahedron shares edges with six surrounding units by positioning one Se atom sharing between three neighboring RE^{3+} ions pointing along the *c*-axis. The polyhedral structural representation is shown in Figure SI 2 in the SI. This interesting connectivity between *RE*Se_6 units creates an infinite triangular lattice of RE^{3+} ions in the *ab*-plane, being displayed in Figure SI 3 in the SI. Moreover, *RE* atoms are sitting in the corners of the unit cell on *ab*-plane (Figure 2) in both structure types; therefore, the distance between RE^{3+} ions is the same as the size of the *a*-axis, which is solely dependent on the size of the RE^{3+} cation (see Figure SI 5 in the Supporting Information). Since the only structural change is that observed within the triangular layer, the Cs*RE*Se_2 series allows one to understand the role of RE^{3+} ions within the same structural motifs, *RE*-ion-dependent crystal electric field (CEF) anisotropy, and the exotic magnetic ground state that may be generated from the lattice frustrations.

The temperature dependence of the magnetization parallel and perpendicular to the *ab*-plane above 2 K for the Cs*RE*Se_2 (*RE* = Ce, Pr, Nd, Sm, Tb, Dy, Er, Tm, Yb) series (see Figure SI 9 in the SI) indicates no long-range magnetic order above 2 K. All these materials show paramagnetic behavior with antiferromagnetic interaction. Large anisotropy was found between *ab*-plane versus *c*-axis magnetization in the Cs*RE*Se_2. Considering the relative high values of $|\theta_{CW}|$, strong frustrated phenomenon is expected in this family. Detailed discussions of magnetic susceptibility, Curie-Weiss fittings, and isothermal magnetizations are given in the SI.

Moreover, we performed AC (DC 0 T, AC 2.5 Oe) and DC (0.2 T) magnetic susceptibility measurement below 2 K for the Kramer ions (Figure 3), where the crystal electric field (CEF) could split the multiplet into the Kramer doublets. The slopes of DC and AC susceptibility of $CsCeSe_2$ both change at 0.7 K, while there is no difference between zero-field cooling (ZFC) and field cooling (FC), and no frequency dependence of AC susceptibility from 1 Hz to 757 Hz. Considering the relatively high first excited energy in Ce^{3+} from the CEF,[44] the slope change at 0.7 K of $CsCeSe_2$ could be caused by the short-range

DOI: 10.1021/acsmaterialslett.9b00464
ACS Materials Lett. 2020, 2, 71−75

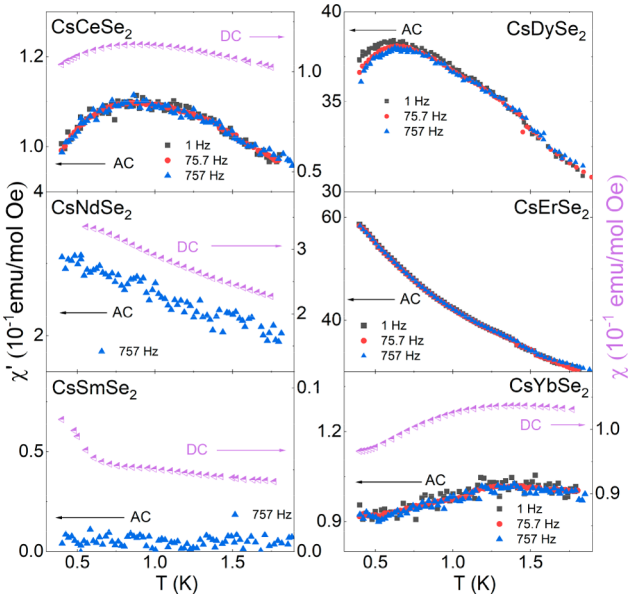

Figure 3. AC and DC magnetic susceptibility below 2 K for the Kramer ions (Ce, Nd, Sm, Dy, Er, and Yb).

magnetic interactions. For $CsNdSe_2$, no magnetic transition is observed in both AC and DC susceptibility down to 0.4 K. The behavior of DC susceptibility deviates from Curie Weiss law, and there is no difference between ZFC and FC. The DC susceptibility of $CsSmSe_2$ exhibits an upturn at 0.6 K. Considering the multilevel CEF for Sm^{3+} and no λ anomaly at the same temperature in the heat capacity, the reason for this feature is likely low-lying CEF states.[45] A magnetic transition is found in $CsDySe_2$ at 0.7 K in the AC susceptibility. The transition moves to a higher temperature by increasing the frequency from 1 Hz to 757 Hz, strongly indicating the spin freezing at 0.7 K is due to the short-range interaction between Dy^{3+} ions. This feature was also found in other frustrated Dy compounds.[46,47] These suggest possible spin-glass state in $CsDySe_2$. AC susceptibility of $CsErSe_2$ increases with lowering temperature down to 0.4 K. Similar behavior has been observed in the previously reported compounds, $AErSe_2$ (A = Na and K) and $ErMgGaO_4$,[48,49] suggesting a possible spin liquid ground state.

Yb^{3+} triangular lattices in $CsYbSe_2$ are very important for investigating QSL due to the possible $J_{eff} = 1/2$. The $YbSe_6$ environment in $CsYbSe_2$ is close to those in $NaYbO_2$ and $YbMgGaO_4$. It may lead to $CsYbSe_2$ becoming a similar $J_{eff} - 1/2$ triangular frustrated magnet.[17,23−26] Unlike $YbMgGaO_4$, $CsYbSe_2$ exhibits a broad peak at 1.5 K in magnetic susceptibility with no bifurcation in the ZFC and FC. The ground state should not be affected by CEF at such low temperature, since the first excited energy from CEF in similar triangular lattice materials (such as $NaYbO_2$ or $YbMgGaO_4$) is observed at temperatures much higher than 1.5 K.[18,24] Furthermore, no clear difference is observed in AC susceptibility measurements (1−757 Hz). Therefore, we can exclude the possibility of having a spin glass ground state in $CsYbSe_2$.

To investigate the magnetic interaction and CEF effects, we also measured the heat capacity at 0 T down to a temperature of 0.4 K. Figure 4 displays a summary of the heat capacity and calculated entropy for all of the compounds. The heat capacity reaches the classical limit of Dulong−Petit law for a phonon

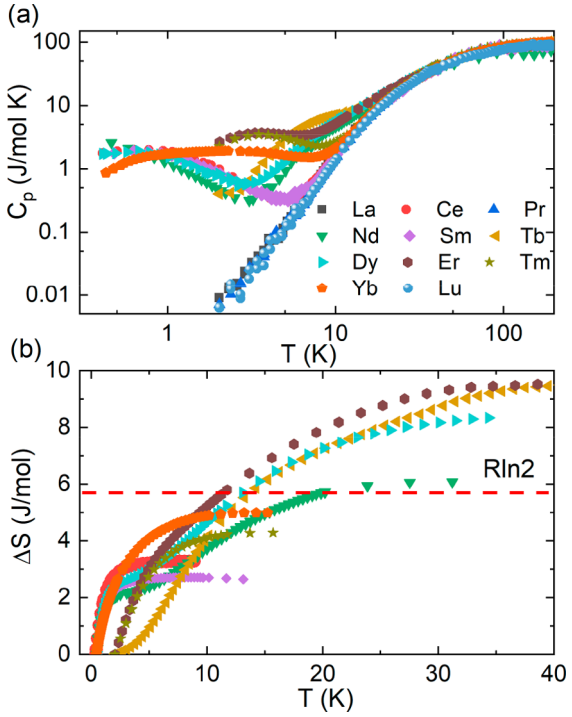

Figure 4. (a) Heat capacity measured at 0 T for Cs*RE*Se_2 series. (b) Calculated magnetic entropy.

heat capacity defined as $3nR = 99.31$ J/(mol K) (where n is the number of atoms per formula unit and R is the gas constant).[50] Because of the full occupied electrons in the outer layers in $CsLaSe_2$ (La^{3+}:$4f^0$) and $CsLuSe_2$ (Lu^{3+}:$4f^{14}$), the heat capacity of $CsLaSe_2$ and $CsLuSe_2$ overlap and provide good phonon references for other compounds. The fitted Debye temperature for $CsLaSe_2$ is 174 K. There is no λ shape anomaly in the heat capacity, indicating no long-range magnetic transition within our measuring temperature range for all compounds. Consistent with the magnetization measurement, the heat capacity results also suggest strong frustrated magnetism in these compounds. The broad peaks were observed in all the compounds except La, Pr, and Lu. We also calculated the entropy from the lowest measurement temperature for each compound. The magnetic entropy of $J_{eff} = 1/2$ should be given as Rln2. $CsNdSe_2$, $CsDySe_2$, $CsTbSe_2$, and $CsErSe_2$ present larger values of the entropy at low temperature, which may be due to the Schottky contributions.[51] Now we focus on $CsCeSe_2$, $CsDySe_2$, and $CsYbSe_2$, which contain downturns in $M(T)$ results. Heat capacity of $CsCeSe_2$ exhibits a broad peak starting from 4 K, which is much lower than the CEF feature in the temperature dependence of the magnetization (see Figure SI 9). With regard to heat capacity, the maximum of the broad peak is observed at a temperature of 0.7 K, which agrees with our magnetization data (see Figure 3). However, the lack of a λ-shaped feature indicates that it may due to short-range magnetic interaction. The magnetic entropy down to a temperature of 0.4 K is 3.4 J/mol, which is 60% of Rln2 in the $S = 1/2$ system. This indicates a possible residual magnetic entropy at lower temperature. Two broad peaks were exhibited in the heat capacity of $CsDySe_2$. The high-temperature broad peak occurs from 3 K to 30 K, whereas no significant anomaly in magnetic susceptibility is observed in the same temperature region, indicating the origin from the Schottky contribution. The low-temperature peak reaches the maximum at 0.7 K,

DOI: 10.1021/acsmaterialslett.9b00464
ACS Materials Lett. 2020, 2, 71−75

further confirming the spin freezing in $CsDySe_2$. In $CsYbSe_2$, there is no λ anomaly near 1.5 K as we observed in the magnetic susceptibility (Figure 3), suggesting a short-range interaction, instead of the long-range magnetic order. A broad peak is observed below 10 K in $CsYbSe_2$, which is similar to $NaYbO_2$. Unlike other *RE* ion compounds, this peak is very broad, implying the spin fluctuation in $CsYbSe_2$.

In this work, new $CsRESe_2$ compounds with an *RE* triangular lattice were discovered, and large single crystals were, for the first time, grown out of the salt flux. Based on the magnetization and heat capacity measurements down to 0.4 K, we found diverse magnetic states in these compounds. $CsDySe_2$ presents the spin-glass state. $CsCeSe_2$ and $CsYbSe_2$ display clear short-range interaction behavior at low temperature. Lack of long-range magnetic order and spin freezing down to 0.4 K in $CsCeSe_2$ and $CsYbSe_2$ suggests their candidacy for quantum spin liquid ground state.

■ ASSOCIATED CONTENT

Supporting Information

The Supporting Information is available free of charge at https://pubs.acs.org/doi/10.1021/acsmaterialslett.9b00464.

Experimental details, tables of crystallographic data, bond lengths, bond angles, temperature-dependent magnetic susceptibility down to 2 K, isothermal magnetizations data, and DFT calculations (PDF)

Accession Codes

CCDC Nos. 1952065−1952075 contain the supplementary crystallographic data for this paper. These data can be obtained free of charge via www.ccdc.cam.ac.uk/data_request/cif, or by emailing data_request@ccdc.cam.ac.uk, or by contacting The Cambridge Crystallographic Data Centre, 12 Union Road, Cambridge CB2 1EZ, UK; fax: +44 1223 336033.

■ AUTHOR INFORMATION

Corresponding Authors

*E-mail: xingj@ornl.gov (J. Xing).
*E-mail: sefata@ornl.gov (A. Sefat).

ORCID

Jie Xing: 0000-0002-9732-2318
Liurukara D. Sanjeewa: 0000-0002-3293-7370
Mao-Hua Du: 0000-0001-8796-167X
Radu Custelcean: 0000-0002-0727-7972

Author Contributions

▽These authors contributed equally.

Notes

The authors declare no competing financial interest.

■ ACKNOWLEDGMENTS

The research is supported by the U.S. Department of Energy (DOE), Office of Science, Basic Energy Sciences (BES), Materials Science and Engineering Division. The X-ray diffraction analysis by R.C. was supported by the U.S. Department of Energy, Office of Science, Basic Energy Sciences, Chemical Sciences, Geosciences, and Biosciences Division. Work at Florida by J.S.K. and G.R.S. was supported by the U.S. Department of Energy, Basic Energy Sciences (Contract No. DE-FG02-86ER45268). This manuscript has been authored by UT-Battelle, LLC, under Contract No. DE-AC05-00OR22725 with the U.S. Department of Energy. The U.S. Government retains and the publisher, by accepting the article for publication, acknowledges that the U.S. Government retains a non-exclusive, paid-up, irrevocable, world-wide license to publish or reproduce the published form of this manuscript, or allow others to do so, for U.S. Government purposes. The Department of Energy will provide public access to these results of federally sponsored research in accordance with the DOE Public Access Plan.

■ REFERENCES

(1) Zhou, Y.; Kanoda, K.; Ng, T. K. Quantum Spin Liquid States. *Rev. Mod. Phys.* **2017**, *89*, No. 025003.
(2) Savary, L.; Balents, L. Quantum Spin Liquids: A Review. *Rep. Prog. Phys.* **2017**, *80*, No. 016502.
(3) Jiang, H.-C.; Wang, Z.; Balents, L. Identifying Topological Order by Entanglement Entropy. *Nat. Phys.* **2012**, *8*, 902.
(4) Kitaev, A. Y. Fault-tolerant Quantum Computation by Anyons. *Ann. Phys.* **2003**, *303*, 2−30.
(5) Yamashita, S.; Nakazawa, Y.; Oguni, M.; Oshima, Y.; Nojiri, H.; Shimizu, Y.; Miyagawa, K.; Kanoda, K. Thermodynamic Properties of a Spin-1/2 Spin-Liquid State in a κ-type Organic Salt. *Nat. Phys.* **2008**, *4*, 459−462.
(6) Itou, T.; Oyamada, A.; Maegawa, S.; Tamura, M.; Kato, R. Quantum Spin Liquid in the Spin-1/2 Triangular Antiferromagnet $EtMe_3Sb[Pd(dmit)_2]_2$. *Phys. Rev. B: Condens. Matter Mater. Phys.* **2008**, *77*, 104413.
(7) Shirata, Y.; Tanaka, H.; Matsuo, A.; Kindo, K. Experimental Realization of a Spin-1/2 Triangular-Lattice Heisenberg Antiferromagnet. *Phys. Rev. Lett.* **2012**, *108*, No. 057205.
(8) Susuki, T.; Kurita, N.; Tanaka, T.; Nojiri, H.; Matsuo, A.; Kindo, K.; Tanaka, H. Magnetization Process and Collective Excitations in the $S = 1/2$ Triangular-Lattice Heisenberg Antiferromagnet $Ba_3CoSb_2O_9$. *Phys. Rev. Lett.* **2013**, *110*, 267201.
(9) Ma, J.; Kamiya, Y.; Hong, T.; Cao, H. B.; Ehlers, G.; Tian, W.; Batista, C.D.; Dun, Z. L.; Zhou, H. D.; Matsuda, M. Static and Dynamical Properties of the Spin-1/2 Equilateral Triangular-Lattice Antiferromagnet $Ba_3CoSb_2O_9$. *Phys. Rev. Lett.* **2016**, *116*, No. 087201.
(10) Itou, T.; Oyamada, A.; Maegawa, S.; Tamura, M.; Kato, R. Quantum Spin Liquid in the Spin-1/2 Triangular Antiferromagnet $EtMe_3Sb[Pd(dmit)_2]_2$. *Phys. Rev. B: Condens. Matter Mater. Phys.* **2008**, *77*, 104413.
(11) Shimizu, Y.; Miyagawa, K.; Kanoda, K.; Maesato, M.; Saito, G. Spin Liquid State in an Organic Mott Insulator with a Triangular Lattice. *Phys. Rev. Lett.* **2003**, *91*, 107001.
(12) Cui, Y.; Dai, J.; Zhou, P.; Wang, P. S.; Li, T. R.; Song, W. H.; Wang, J. C.; Ma, L.; Zhang, Z.; Li, S. Y.; et al. Mermin-Wagner Physics, (H,T) Phase Diagram, and Candidate Quantum Spin-Liquid Phase in the Spin-1/2 Triangular-Lattice Antiferromagnet $Ba_8CoNb_6O_{24}$. *Phys. Rev. Mater.* **2018**, *2*, No. 044403.
(13) Clarke, S. J.; Fowkes, A. J.; Harrison, A.; Ibberson, R. M.; Rosseinsky, M. J. Synthesis, Structure, and Magnetic Properties of $NaTiO_2$. *Chem. Mater.* **1998**, *10*, 372−384.
(14) Witczak-Krempa, W.; Chen, G.; Kim, Y.B.; Balents, L. Correlated quantum phenomena in the strong spin-orbit regime. *Annu. Rev. Condens. Matter Phys.* **2014**, *5*, 57−82.
(15) Balents, L. Spin Liquids in Frustrated Magnets. *Nature* **2010**, *464*, 199−208.
(16) Gardner, J. S.; Gingras, M. J.; Greedan, J. E. Magnetic Pyrochlore Oxides. *Rev. Mod. Phys.* **2010**, *82*, 53.
(17) Li, Y.; Liao, H.; Zhang, Z.; Li, S.; Jin, F.; Ling, L.; Zhang, L.; Zou, Y.; Pi, L.; Yang, Z.; et al. Gapless Quantum Spin Liquid Ground State in the Two-Dimensional Spin-1/2 Triangular Antiferromagnet $YbMgGaO_4$. *Sci. Rep.* **2015**, *5*, 16419.
(18) Li, Y.; Chen, G.; Tong, W.; Pi, L.; Liu, J.; Yang, Z.; Wang, X.; Zhang, Q. Rare-earth Triangular Lattice Spin Liquid: a Single-Crystal Study of $YbMgGaO_4$. *Phys. Rev. Lett.* **2015**, *115*, 167203.
(19) Li, Y.; Adroja, D.; Biswas, P. K.; Baker, P. J.; Zhang, Q.; Liu, J.; Tsirlin, A. A.; Gegenwart, P.; Zhang, Q. Muon Spin Relaxation Evidence for the U(1) Quantum Spin-Liquid Ground State in the

DOI: 10.1021/acsmaterialslett.9b00464
ACS Materials Lett. 2020, 2, 71−75

Triangular Antiferromagnet $YbMgGaO_4$. *Phys. Rev. Lett.* **2016**, *117*, No. 097201.
(20) Shen, Y.; Li, Y. D.; Wo, H.; Li, Y.; Shen, S.; Pan, B.; Wang, Q.; Walker, H. C.; Steffens, P.; Boehm, M.; et al. Evidence for a Spinon Fermi Surface in a Triangular-Lattice Quantum-Spin-Liquid Candidate. *Nature* **2016**, *540*, 559−562.
(21) Paddison, J. A.; Daum, M.; Dun, Z.; Ehlers, G.; Liu, Y.; Stone, M. B.; Zhou, H.; Mourigal, M. Continuous Excitations of the Triangular-Lattice Quantum Spin Liquid $YbMgGaO_4$. *Nat. Phys.* **2017**, *13*, 117−122.
(22) Liu, W.; Zhang, Z.; Ji, J.; Liu, Y.; Li, J.; Wang, X.; Lei, H.; Chen, G.; Zhang, Q. Rare-earth Chalcogenides: A Large Family of Triangular Lattice Spin Liquid Candidates. *Chin. Phys. Lett.* **2018**, *35*, 117501.
(23) Baenitz, M.; Schlender, P.; Sichelschmidt, J.; Onykiienko, Y. A.; Zangeneh, Z.; Ranjith, K. M.; Sarkar, R.; Hozoi, L.; Walker, H. C.; Orain, J.C.; et al. $NaYbS_2$: A Planar Spin-1/2 Triangular-Lattice Magnet and Putative Spin Liquid. *Phys. Rev. B: Condens. Matter Mater. Phys.* **2018**, *98*, 220409.
(24) Ding, L.; Manuel, P.; Bachus, S.; Grußler, F.; Gegenwart, P.; Singleton, J.; Johnson, R. D.; Walker, H. C.; Adroja, D. T.; Hillier, A. D.; Tsirlin, A. A. Gapless Spin-Liquid State in the Structurally Disorder-free Triangular Antiferromagnet $NaYbO_2$. *Phys. Rev. B: Condens. Matter Mater. Phys.* **2019**, *100*, 144432.
(25) Ranjith, K. M.; Dmytriieva, D.; Khim, S.; Sichelschmidt, J.; Luther, S.; Ehlers, D.; Yasuoka, H.; Wosnitza, J.; Tsirlin, A. A.; Kühne, H.; Baenitz, M. Field-induced Instability of the Quantum Spin Liquid Ground State in the J_{eff} = 1/2 Triangular-lattice Compound $NaYbO_2$. *Phys. Rev. B: Condens. Matter Mater. Phys.* **2019**, *99*, 180401.
(26) Bordelon, M. M.; Kenney, E.; Liu, C.; Hogan, T.; Posthuma, L.; Kavand, M.; Lyu, Y.; Sherwin, M.; Butch, N. P.; Brown, C.; et al. Field-tunable Quantum Disordered Ground State in the Triangular Lattice Antiferromagnet $NaYbO_2$. *Nat. Phys.* **2019**, *15*, 1058−1064.
(27) Cantwell, J. R.; Roof, I. P.; Smith, M. D.; zur Loye, H.-C. Crystal Growth and Optical Properties of Lithium−Lanthanide Oxides: $LiLnO_2$ (*Ln* = Nd, Sm, Eu, Gd and Dy). *Solid State Sci.* **2011**, *13*, 1006−1012.
(28) Hashimoto, Y.; Wakeshima, M.; Hinatsu, Y. Magnetic properties of ternary sodium oxides $NaLnO_2$ (*Ln* = rare earths). *J. Solid State Chem.* **2003**, *176*, 266−272.
(29) Hoppe, R.; Kroeschell, P.; Wolf, R. Notiz über den α-$LiFeO_2$-Type: $NaPrO_2$ und $NaTbO_2$. *Z. Anorg. Allg. Chem.* **1986**, *537*, 97.
(30) Brunn, H.; Hoppe, R. Neue ternäre Oxide der Seltenen Erden: Über $RbSEO_2$ (SE = La, Nd, Sm, Eu, Gd) sowie $CsNdO_2$. *Z. Anorg. Allg. Chem.* **1975**, *417*, 213.
(31) Miyasaka, N.; Doi, Y.; Hinatsu, Y. Synthesis and Magnetic Properties of $ALnO_2$ (*A* = Cu or Ag; *Ln* = Rare-earths) with the Delafossite Structure. *J. Solid State Chem.* **2009**, *182*, 2104−2110.
(32) Deng, B.; Ellis, D. E.; Ibers, J. A. New Layered Rubidium Rare-earth Selenides: Syntheses, Structures, Physical Properties, and Electronic Structures for $RbLnSe_2$. *Inorg. Chem.* **2002**, *41*, 5716−5720.
(33) Dong, B.; Doi, Y.; Hinatsu, Y. Structure and Magnetic Properties of Ternary Potassium Lanthanide Oxides $KLnO_2$ (*Ln* = Y, Nd, Sm−Lu). *J. Alloys Compd.* **2008**, *453*, 282−287.
(34) Ohtani, T.; Honjo, H.; Wada, H. Synthesis, Order-disorder Transition and Magnetic Properties of $LiLnS_2$, $LiLnSe_2$, $NaLnS_2$ and $NaLnSe_2$ (*Ln* = Lanthanides). *Mater. Res. Bull.* **1987**, *22*, 829−840.
(35) Havlak, L.; Fábry, J.; Henriques, M.; Dušek, M. Structure Determination of $KScS_2$, $RbScS_2$ and $KLnS_2$ (*Ln* = Nd, Sm, Tb, Dy, Ho, Er, Tm and Yb) and Crystal−Chemical Discussion. *Acta Crystallogr., Sect. C: Struct. Chem.* **2015**, *71*, 623−630.
(36) Bronger, W.; Brüggemann, W.; Von der Ahe, M.; Schmitz, D. Zur Synthese und Struktur ternärer Chalcogenide der Seltenen Erden $ALnX_2$ mit *A*≙ alkalimetall und *X*≙ Schwefel, Selen oder Tellur. *J. Alloys Compd.* **1993**, *200*, 205−210.
(37) Zhu, Z.; Maksimov, P. A.; White, S. R.; Chernyshev, A. L. Disorder-Induced Mimicry of a Spin Liquid in $YbMgGaO_4$. *Phys. Rev. Lett.* **2017**, *119*, 157201.
(38) Xu, Y.; Zhang, J.; Li, Y. S.; Yu, Y. J.; Hong, X. C.; Zhang, Q. M.; Li, S. Y. Absence of Magnetic Thermal Conductivity in the Quantum Spin-liquid Candidate $YbMgGaO_4$. *Phys. Rev. Lett.* **2016**, *117*, 267202.
(39) Li, Y. $YbMgGaO_4$: A Triangular-Lattice Quantum Spin Liquid Candidate. *Adv. Quantum Technol.* **2019**, 1900089.
(40) Moriya, T. Anisotropic Superexchange Interaction and Weak Ferromagnetism. *Phys. Rev.* **1960**, *120*, 91.
(41) Moriya, T. New Mechanism of Anisotropic Superexchange Interaction. *Phys. Rev. Lett.* **1960**, *4*, 228.
(42) Dzyaloshinsky, I. A Thermodynamic Theory of "Weak" Ferromagnetism of Antiferromagnetics. *J. Phys. Chem. Solids* **1958**, *4*, 241−255.
(43) Deng, B.; Ibers, J.A. $CsYbSe_2$. *Acta Crystallogr., Sect. E: Struct. Rep. Online* **2005**, *61*, i15−i17.
(44) Lee, J.; Rabus, A.; Lee-Hone, N.R.; Broun, D.M.; Mun, E. The two-Dimensional Metallic Triangular Lattice Antiferromagnet $CeCd_3P_3$. *Phys. Rev. B: Condens. Matter Mater. Phys.* **2019**, *99*, 245159.
(45) Wertheim, G.K.; Crecelius, G. Divalent Surface State on Metallic Samarium. *Phys. Rev. Lett.* **1978**, *40*, 813.
(46) Greedan, J. E. Frustrated Rare Earth Magnetism: Spin Glasses, Spin Liquids and Spin ices in Pyrochlore Oxides. *J. Alloys Compd.* **2006**, *408*, 444−455.
(47) Ramirez, A. P. Strongly Geometrically Frustrated Magnets. *Annu. Rev. Mater. Sci.* **1994**, *24*, 453−480.
(48) Xing, J.; Sanjeewa, L. D.; Kim, J.; Meier, W. R.; May, A. F.; Zheng, Q.; Custelcean, R. C.; Stewart, G. R.; Sefat, A. S. Synthesis, Magnetization and Heat Capacity of Triangular Lattice Materials $NaErSe_2$ and $KErSe_2$. *Phys. Rev. Mater.* **2019**, *3*, DOI: 10.1103/PhysRevMaterials.3.114413.
(49) Cai, Y.; Lygouras, C.; Thomas, G.; Wilson, M. N.; Beare, J.; Yahne, D. R.; Ross, K.; Gong, Z.; Uemura, Y. J.; Dabkowska, H. A.; Luke, G. M. μSR Study of Triangular Ising Antiferromagnet $ErMgGaO_4$. *ArXiv preprint*, arXiv:1905.12798, 2019.
(50) Kittel, C. *Introduction to Solid State Physics*. Wiley: New York, 1976.
(51) Mun, E.D.; Bud'ko, S.L.; Ko, H.; Miller, G.J.; Canfield, P.C. Physical properties and anisotropies of the $RNiGe_3$ series (R = Y, Ce−Nd, Sm, Gd−Lu). *J. Magn. Magn. Mater.* **2010**, *322*, 3527−3543.

DOI: 10.1021/acsmaterialslett.9b00464
ACS Materials Lett. 2020, 2, 71−75